

Realizing Photonic Integrated Circuits on Thin Film Lithium Niobate

Parthorn Ammawat

Mentors: Ryoto Sekine and Prof. Alireza Marandi

Abstract: Integrated photonics based on thin film lithium niobate (TFLN) has been a promising all-optical solution for low-cost and energy-efficient communication, sensing, and computing. Due to its strong non-linearity, TFLN has emerged as a promising foundation for modern systems including photonic computing. However, all computers require a combination of linear and nonlinear operations. While these elements have been demonstrated individually on TFLN, they have yet to be combined on the same chip to implement a full computer. To do so requires further optimization of both components to make them compatible with each other. One vital component of the circuits is optical couplers. This project optimized several types of couplers and performed fabrication sensitivity tests on them. These were done by using commercial software, and then the results were verified by using different simulation methods, including FDE, EME, and FDTD. The real devices were then fabricated, and the results were measured.

1 Introduction

Recently, integrated photonics has emerged as a highly promising option for achieving cost-effective and energy-efficient communication, sensing, and computation through an all-optical approach. Among the available materials, thin-film lithium niobate (TFLN), which has recently become commercial, has appeared to be a potential integrated photonic platform since, unlike other popular platforms such as silicon and silicon nitride, lithium niobate exhibits an exceptionally strong nonlinearity that other materials do not have which enables various significant applications, including intense frequency conversion, 100 GHz electro-optics, and multi-octave frequency combs at ~ 100 fJ pump pulse energies¹⁻³. Consequently, photonic circuits on TFLN have emerged as a promising foundation for modern systems including photonic computing, biomedical devices, quantum networks, and telecommunication systems. Among these applications, photonic computing is of high interest to researchers in this field. Compared to conventional electronic computers photonic computing has the potential for orders of magnitude higher computation bandwidth and enables access to different types of computing dynamics and architectures⁴. All computers however require a combination of linear and nonlinear operations⁵. While these elements have been demonstrated individually on TFLN⁶⁻⁷, the integration of both on a single chip to create a full circuit or computer has not been realized yet. To achieve this, further optimization of both elements is necessary to ensure their compatibility.

This project aims to optimize circuits on TFLN for photonic computing, which will potentially allow complex computations, including NP-hard problem-solving and machine learning optimization. The main components of the circuits include electro-optic modulators (EOMs), on-chip heaters, on-chip optical parametric oscillators (OPOs), optical couplers, and inverse tapers. Among these, optical couplers are one of the most critical components. In this work, two main types of couplers, directional and adiabatic couplers, are examined and optimized by using commercial simulation software (Lumerical), and fabrication sensitivity tests are also performed on directional couplers. The optimized results are then verified using different simulation methods (FDE, EME, and FDTD) and data obtained from real fabricated devices. The results from this work would allow for better optimization of the devices being developed in the lab since these couplers are a crucial part of other components.

2 Methods

2.1 Device Design and Optimization

Couplers are designed and optimized using Lumerical, a commercial photonic simulation software. In this project, we focus on the design of 3dB couplers with an intended power coupling of 50%. The materials used for the simulations are 700-nm-thick thin film lithium niobate (TFLN) on silicon dioxide (SiO_2) on silicon (Si) with 1- μm -thick SiO_2 cladding, and light of wavelength 2.126 μm is used. The work concerns two main types of couplers: directional and adiabatic couplers.

2.1.1 Directional Couplers

Directional couplers consist of two identical waveguides with a separation small enough for light in both waveguides to interact and couple. Normally, light is input into one waveguide (input waveguide) and a fraction of light is coupled into the other waveguide (output waveguide). This fraction depends on the geometry of the couplers (separation gap, waveguide width, coupler length, etc.) and the wavelength of light. For directional couplers, the analytic equation governing the power fraction coupled into the output waveguide is $C = \sin^2\left(\frac{\Delta n_{eff}\pi L}{\lambda}\right)$, where Δn_{eff} is the difference in effective indices of the even and odd modes, L is the coupling length, and λ is the wavelength of light⁸. In order to optimize the couplers, Lumerical's finite-difference eigenmode (FDE) solver, which calculates the modes' spatial profile and frequency dependence by solving Maxwell's equations in two dimensions on a cross-sectional mesh of the structure, is used to calculate Δn_{eff} for a particular geometry, and, with a desired coupling power, the length of the coupler can be calculated.

To begin with, the waveguide width of 1.65 μm is chosen since this is the width that has already been optimized for systems with the same material structure. The separation gap of 800 nm is selected because it is large enough to avoid overlapping of the waveguides from fabrication errors, and it is small enough to allow interaction of light in both waveguides. Thus, the value to be obtained for optimization is the coupler length. After the optimized parameters from FDE are obtained, two more powerful and more expensive simulation methods, eigenmode expansion (EME), which divides the three-dimensional structure into multiple cells and uses FDE to solve for the modes at the interfaces of adjacent cells, and finite-difference time-domain (FDTD), which directly solves the time-dependent Maxwell's equations without any physical approximations and is limited only by the extent of the computing power available, are used to simulate the optimized parameters since these two simulation methods can give more accurate results if there is enough computing power. The results are then compared to verify the optimized design.

Finally, the fabrication tolerance tests are performed on the optimized design by varying light wavelength, waveguide width, etch depth, sidewall angle, and thin film thickness. The ranges of deviations are chosen to be within the maximum typical errors encountered in real fabricated devices, which are 0.1 μm for light wavelength, 0.05 μm for waveguide width, 20 nm for etch depth, 10 degrees for sidewall angle, and 10 nm of thin film thickness. Due to its cost and time efficiencies, FDE is used for the tests.

2.1.2 Adiabatic Couplers

Adiabatic couplers consist of two asymmetric waveguides with different initial widths. For 3dB adiabatic couplers, both waveguides are tapered to the same final width that is equal to the average widths, and the widths must change slowly enough for the adiabatic transition to occur. Unlike directional couplers, adiabatic couplers do not have an exact analytic equation governing the coupling factor, so only EME and FDTD, which do not require exact equations, can be used.

Similar to directional couplers, different waveguide widths that have an average of 1.65 μm are tested, and a gap of 1000 nm is selected to satisfy the adiabatic conditions. The width pair with the smallest difference that enables adiabatic processes is then chosen. Finally, the length is optimized. These are done

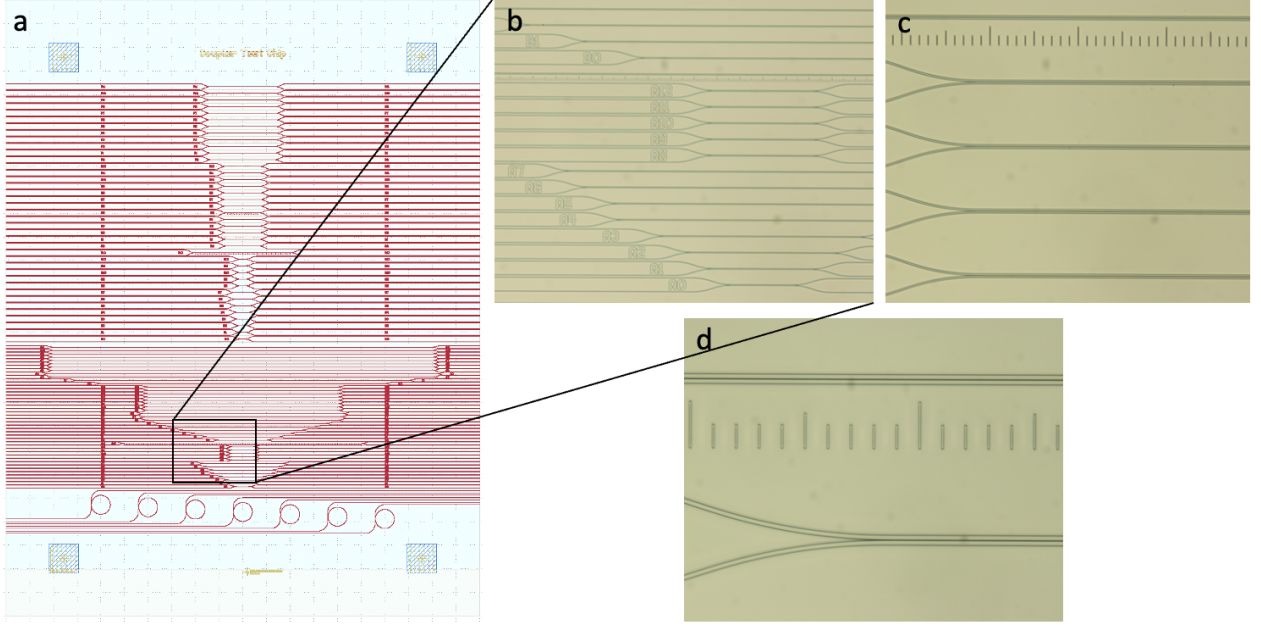


Figure 1: Design of the chip. **a)** The designed pattern. **b), c), and d)** The fabricated pattern observed under an optical microscope.

using EME because FDTD requires much more computing power and time - approximately 20 GB of memory and 30 hours, respectively, per simulation - since it needs to solve Maxwell's equations in both space and time domains using miniature steps. After the optimized parameters are obtained from EME, FDTD is used to confirm the results.

2.2 Device Fabrication

To verify the results obtained from the simulations, I fabricated both types of couplers with varying lengths (see appendix), as shown in figure 1, onto a TFLN on insulator (LNOI) chip. The coupling factors will be measured for each length and then compared to the simulated results. The chip consists of 700-nm-thick TFLN on 4.7- μm -thick SiO_2 on 500- μm -thick Si. The fabrication process starts with cleaning the chip then spin-coating HSQ (a negative electron-beam resist) onto the top surface of the chips. Next, I patterned the chip by using electron beam. After that, I developed the chip using TMAH before etching it with plasma etching. I then remove the resist and finally coat the device with 1- μm -thick of SiO_2 as a cladding layer.

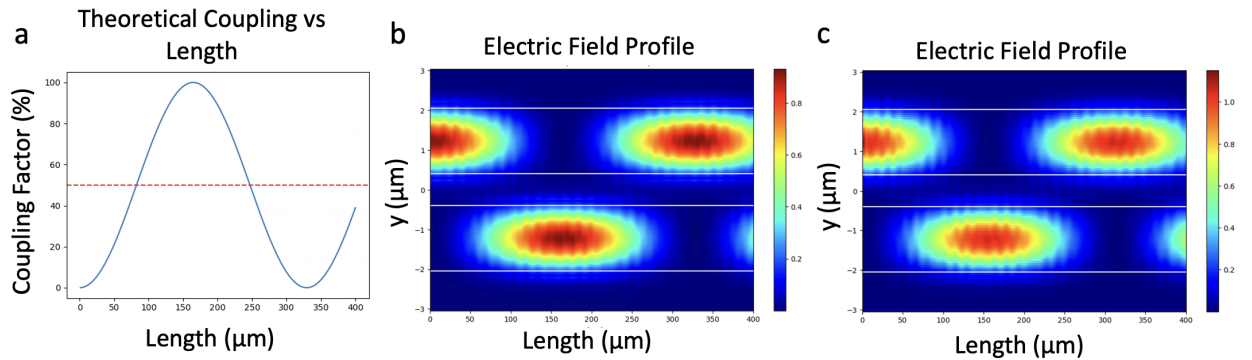


Figure 2: Simulation results for directional couplers of length 400 μm from **a)** FDE, **b)** EME, and **c)** FDTD. The white lines indicate the boundaries of the waveguides.

3 Results

3.1 Directional Couplers

The simulation results for directional couplers are shown in figure 2. The shortest lengths that give a 50% coupling factor are $82.3\text{ }\mu\text{m}$, $82.4\text{ }\mu\text{m}$, and $78\text{ }\mu\text{m}$ for FDE, EME, and FDTD, respectively. The plot comparing coupling factors to the length of $82.4\text{ }\mu\text{m}$ from different simulation methods is illustrated in figure 3. The discrepancy in the results comes from the way the simulations work and the resolutions used. For FDE and EME, the results are very close since both solve Maxwell's equations in two dimensions with the same spatial resolution of 20 nm . On the other hand, FDTD solves Maxwell's equations in three dimensions in both space and time domains, and due to limited computing power, the highest spatial resolution that can be used is only 50 nm . Combining this with errors that occur from using time steps results in lower accuracy. This implies that in general, FDTD gives lower accuracy compared to the other methods, although it can be used to simulate more complicated structures that other methods cannot. One way to increase the accuracy of FDTD is by increasing the resolution, in both space and time domains, but this will also increase the required memory and time for simulations.

The results from the fabrication tolerance tests are also shown in figure 4. It can be seen that directional couplers are somewhat sensitive to variations in light wavelength, waveguide top width, and etch depth, with coupling factors altering within 5%. On the other hand, they are highly sensitive to sidewall angles with coupling factors deviating from lower than 35% to higher than 80%, while they are insensitive to thin film thickness with coupling factors fluctuating less than 2%.

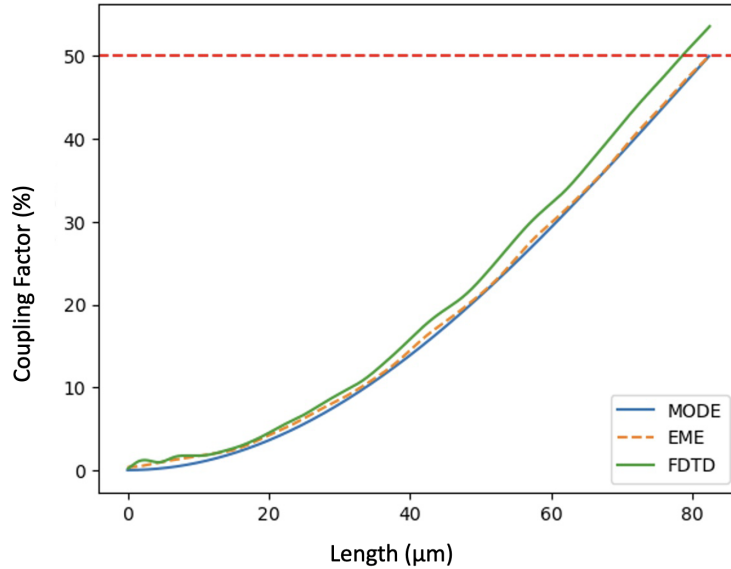


Figure 3: Comparison of coupling factors for different simulation methods up to the longest optimal length ($82.4\text{ }\mu\text{m}$) for directional couplers.

3.2 Adiabatic Couplers

The EME and FDTD simulations for adiabatic couplers are shown in figure 5. Both methods give very similar results, but EME gives a much smoother and higher-resolution profile. Since adiabatic couplers are more complicated and are much longer than directional couplers, the highest allowed resolution is only 100 nm for FDTD, which drastically decreases the smoothness of the field profile and thus the accuracy of the simulation. This can also quantitatively be seen in the comparison plots of the coupling factors in figure 6: the variations of the coupling factors with lengths have the same pattern with small discrepancies, and the

final coupling factors differ by approximately 3%.

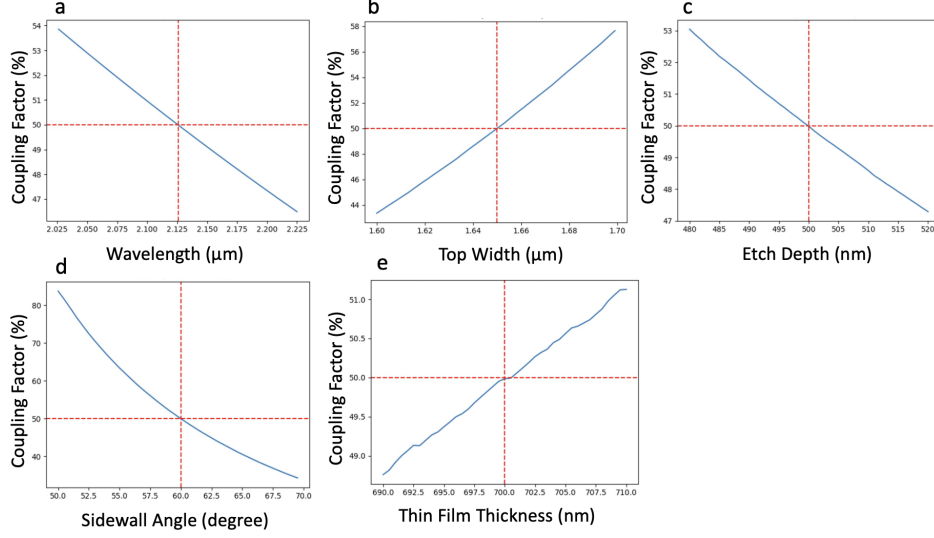


Figure 4: Fabrication tolerance test results for **a)** light wavelength, **b)** waveguide top width, **c)** etch depth, **d)** sidewall angle, and **e)** thin film thickness.

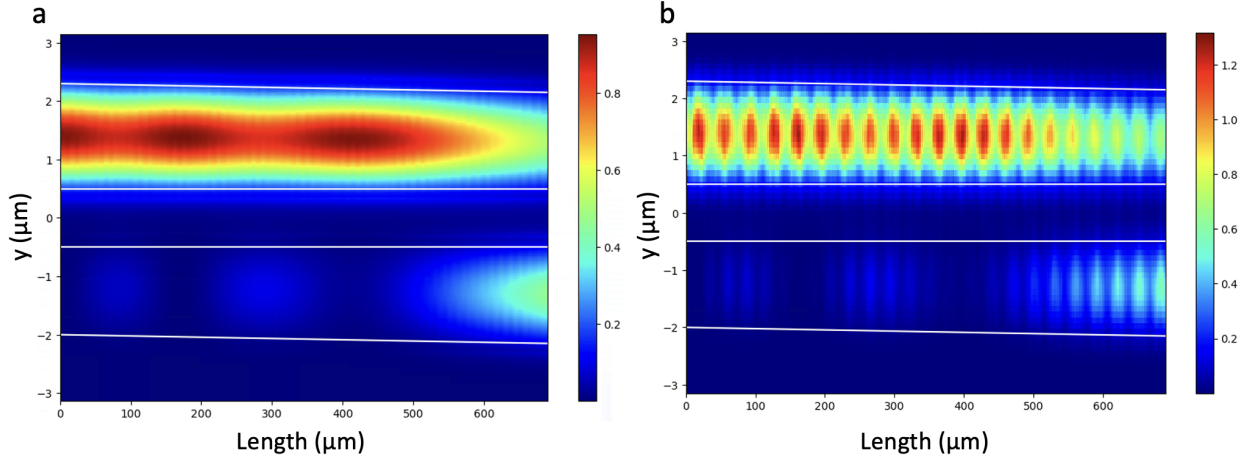


Figure 5: Simulation results for adiabatic couplers of the optimized length $690\ \mu\text{m}$ from **a)** EME and **b)** FDTD. The white lines indicate the boundaries of the waveguides.

4 Conclusions

In conclusion, we have successfully optimized directional and adiabatic couplers with a 50-50 power splitting ratio. For a wavelength of $2.126\ \mu\text{m}$, the lengths of the couplers were found to be $82\ \mu\text{m}$ and $690\ \mu\text{m}$ for directional and adiabatic couplers, respectively. In addition, the results from different simulation methods, including FDE, EME, and FDTD, are in good agreement, and the real devices containing both types of couplers with different parameters were fabricated. Furthermore, fabrication tolerance tests were also performed on directional couplers. Following this work, the optimized results can be further verified by performing measurements on the real fabricated devices, and fabrication tolerance tests can also be performed on adiabatic couplers in the same way. This will allow for comparison of the fabrication robustness between directional and adiabatic couplers, which can potentially enable better optimization of other devices

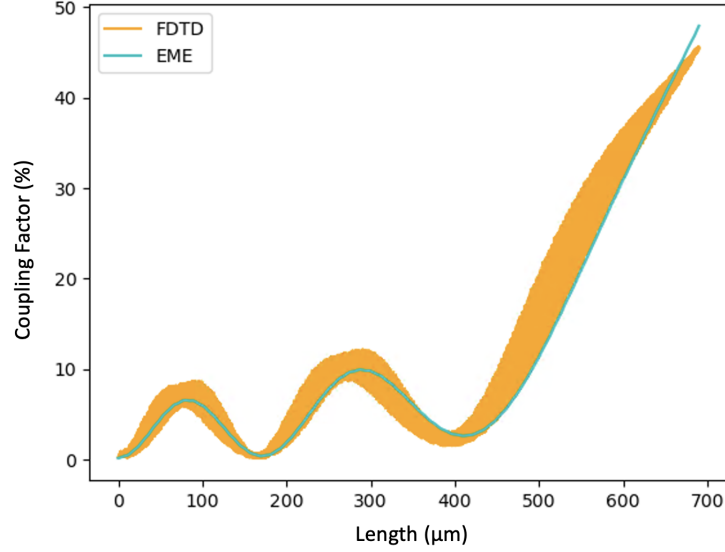


Figure 6: Comparison of coupling factors for different simulation methods up to 690 μm for adiabatic couplers.

and ultimately realize an all-optical on-chip photonic circuit.

Acknowledgements: I would like to thank my mentors, Ryoto Sekine and Alireza Marandi, for their invaluable guidance and support throughout this project. In addition, I would like to express my gratitude to Guy DeRose for signing me off on electron beam lithography and Lena Wolff for training me on scanning electron microscopy. Finally, I gratefully acknowledge facility support from the Kavli Nanoscience Institute (KNI) at Caltech, where I was trained and learned how to fabricate chips and where device nanofabrication was performed.

References

1. Boes, A., Chang, L., Langrock, C., Yu, M., Zhang, M., Lin, Q., Lončar, M., Fejer, M., Bowers, J., & Mitchell, A. (2023). Lithium niobate photonics: Unlocking the electromagnetic spectrum. *Science*, 379(6627). <https://doi.org/10.1126/science.abj4396>.
2. Zhu, D., Shao, L., Yu, M., Cheng, R., Desiatov, B., Xin, C. J., Hu, Y., Holzgrafe, J., Ghosh, S., Shams-Ansari, A., Puma, E., Sinclair, N., Reimer, C., Zhang, M., & Lončar, M. (2021). Integrated photonics on thin-film lithium niobate. *Advances in Optics and Photonics*, 13(2), 242. <https://doi.org/10.1364/aop.411024>.
3. Sekine, Ryoto, et al. “Multi-octave frequency comb from a nanophotonic parametric oscillator.” *Optica Nonlinear Optics Topical Meeting 2023*, 2023, <https://doi.org/10.1364/nlo.2023.w3a.5>.
4. Sekine, R., Li, G., Parto, M., & Marandi, A. (2022). Some computing problems photonics can do best. [Unpublished manuscript].
5. Van der Sande, Guy, et al. “Advances in photonic reservoir computing.” *Nanophotonics*, vol. 6, no. 3, 2017, pp. 561-576, <https://doi.org/10.1515/nanoph-2016-0132>.
6. Guo, Q., Sekine, R., Ledezma, L., Nehra, R., Dean, D. J., Roy, A., Gray, R. M., Jahani, S., & Marandi, A. (2022). Femtojoule femtosecond all-optical switching in lithium niobate nanophotonics. *Nature Photonics*, 16(9), 625-631. <https://doi.org/10.1038/s41566-022-01044-5>.

7. Nehra, Rajveer, et al. “Few-cycle vacuum squeezing in Nanophotonics.” *Science*, vol. 377, no. 6612, 2022, pp. 1333-1337, <https://doi.org/10.1126/science.abo6213>.
8. Osgood, Richard, and Xiang Meng. “Optical Couplers.” *Principles of Photonic Integrated Circuits: Materials, Device Physics, Guided Wave Design*, Springer, Cham, 2022.

Appendix

The devices fabricated on the test chip are listed in table 1 and 2 for directional and adiabatic couplers, respectively. The devices also have the following properties:

- Number of copies for each set of parameters: 5
- Distance between each device: $2\ \mu\text{m}$

WG 1 Width (μm)	WG 2 Width (μm)	Length (μm)	Expected Coupling Factor (%)
1.65	1.65	50	21.1
1.65	1.65	82.3	50
1.65	1.65	100	66.6
1.65	1.65	165	100
1.65	1.65	200	89
1.65	1.65	247	50
1.65	1.65	300	7.6
1.65	1.65	330	0
1.62	1.62	82.3	46
1.62	1.65	82.3	49.6
1.62	1.68	82.3	49.6
1.65	1.68	82.3	53.7
1.68	1.68	82.3	54.5
1.65	1.65	2000 + Ruler	For Visualization

Table 1: This table lists the sets of parameters of the directional couplers fabricated on the test chip. The gap between the waveguides is fixed at 800 nm

w1 (μm)	w2 (μm)	End Width 1 (μm)	End Width 2 (μm)	Length (μm)
1.8	1.5	1.65	1.65	650
1.8	1.5	1.65	1.65	660
1.8	1.5	1.65	1.65	670
1.8	1.5	1.65	1.65	680
1.8	1.5	1.65	1.65	690
1.8	1.5	1.65	1.65	650 + Ruler (gap = $2.25\ \mu\text{m}$)
1.8	1.55	1.65	1.7	690
1.8	1.45	1.65	1.6	690
1.85	1.5	1.7	1.65	690
1.85	1.55	1.7	1.7	690
1.85	1.45	1.7	1.6	690
1.75	1.5	1.6	1.65	690
1.75	1.55	1.6	1.7	690
1.75	1.45	1.6	1.6	690

Table 2: This table lists the sets of parameters of the 3dB adiabatic couplers fabricated on the test chip. The gap between the waveguides is fixed at 1000 nm